Experimental and Microstructural Investigation on the Influence of Cement Type and Brick Type on the Bond Strength of Masonry

[1]Neerukonda Ravi Teja, [2]Korakuti Hanumanth, [3]Rani Naga Satya Syamala, [4]Vipparthi Anitha, [5]Pullagura Rajesh

[1]M.Tech Student, [2]Associate Professor, [3,4,5]Assistant Professor
[1,2,3,4,5] Department of Civil Engineering,
[1,2,3,4,5]Bonam Venkata Chalamayya Engineering College (Autonomous), Odalarevu, Andhra Pradesh, India.

Abstract: This thesis presents a systematic investigation into the fresh-state properties, macro-mechanical performance, and microstructural phase configurations of structural masonry assemblages. Utilizing a 3 x 3 full factorial experimental design, the research evaluates three regional masonry units (country/handmade clay, machine-made wire-cut clay, and pressed fly ash bricks) paired with three commercial cement binders (Ordinary Portland Cement Grade 53, Portland Pozzolana Cement, and Portland Slag Cement) under a standardized water-to-cement ratio of 0.55 and a uniform 10 mm mortar joint thickness.

Fresh-state evaluations revealed that fly ash-based PPC mortars optimize consistency and workability due to the spherical "ball-bearing" effect of pozzolanic grains. Destructive structural testing at a 28-day curing age established that the masonry unit type dominates axial compressive strength (F = 1265.87), with high-density machine-made brick prisms achieving peak capacities up to 6.60 N/mm2 by resisting lateral tensile splitting. Conversely, interfacial flexural tensile bond strength is driven by a highly significant interaction effect (F = 6.86).

X-ray Diffraction (XRD) analysis isolated the underlying chemical kinetics within the Interfacial Transition Zone (ITZ). High-absorption handmade units dewater the fresh paste, forming a weak plane dominated by large, oriented portlandite crystals (0.12 N/mm2 bond). Meanwhile, the active pozzolanic silica within fly ash substrates consumes calcium hydroxide, replacing weak crystalline layers with a dense secondary calcium silicate hydrate (C-S-H) gel matrix that optimizes adhesive bond efficiency (0.52 N/mm2). These findings provide local engineers with clear, scientifically backed guidance for selecting compatible material combinations to maximize masonry durability.

Key Words: Flexural tensile strength, Compressive Strength of Masonry, Initial rate of water absorption, Brick, Cement Types

1. INTRODUCTION

Structural masonry remains one of the oldest and most widely utilized construction typologies globally, owing to its economic viability, thermal efficiency, and structural versatility. As a highly heterogeneous composite material, the global mechanical behavior of a masonry element is dictated by the individual engineering properties of its distinct constituents—namely, the masonry unit and the mortar binder—and, more critically, the complex physical and chemical interaction occurring at their interface. In developing regions, such as the Indian subcontinent, the construction sector frequently utilizes a diverse array of locally sourced and industrially manufactured materials. This variation includes traditional country/handmade clay bricks, modern machine-made wire-cut clay bricks, and factory-pressed hydraulic fly ash bricks, paired across varying projects with Ordinary Portland Cement (OPC), Portland Pozzolana Cement (PPC), or Portland Slag Cement (PSC) (Sarangapani et al., 2005).

Despite its widespread application, predicting the ultimate limit states of composite masonry assemblages under structural loads remains a persistent challenge for structural engineers. Standard design frameworks often simplify masonry design by applying empirical codes that estimate composite compressive capacity primarily as a linear function of individual unit strength. However, this approach frequently ignores the multi-variable interaction kinetics and stiffness mismatches that generate localized internal stress states under axial loading. Under compressive actions, the mortar joint—characterized by a lower elastic modulus than a high-density brick—tends to expand laterally more than the adjacent units. This lateral expansion is restrained by the unit-mortar bond, placing the mortar joint under triaxial compression while subjecting the masonry units to lateral bilateral tension (Costigan & Pavía, 2013). Consequently, the ultimate failure of the system is often initiated by lateral splitting or cracking within the unit or along the joint interface, rather than simple crushing.

Furthermore, the flexural tensile bond strength represents a critical baseline metric for structural integrity against lateral hazards, such as seismic or wind actions. This parameter is directly governed by the microstructure of the Interfacial Transition Zone (ITZ), which spans a narrow gradient (typically <50μm) from the substrate surface (Lawrence & Cao, 1987). The mineralogical development within this zone is highly sensitive to the transport of moisture during the first few minutes of contact. High-absorption units can aggressively dewater fresh plastic paste, starving cement grains of the moisture needed for hydration and leaving behind a porous interface dominated by large, weak, and highly oriented portlandite ($Ca(OH)_2$) crystals (Oliveira et al., 2012).

Conversely, incorporating supplementary cementitious materials (SCMs)—such as the fly ash present in PPC binders or pressed fly ash bricks—can fundamentally alter this microstructural environment. Active pozzolanic particles near the contact zone chemically consume local calcium hydroxide, replacing weak crystalline layers with a dense, interconnected network of secondary calcium silicate hydrate (C-S-H) gel (Venkatarama Reddy & Gupta, 2008).

While the individual materials are well-documented, a clear research gap remains regarding how these variables systematically interact within a full factorial experimental framework. This study addresses this gap by executing a 3 x 3 full factorial program combined with Two-Way Analysis of Variance (ANOVA) and X-ray Diffraction (XRD) tracking to map the micro-to-macro mechanical pathways governing bond efficiency and structural capacity.

2. LITERATURE SURVEY

The structural integrity of unreinforced masonry assemblages relies fundamentally on the quality of the bond developed between the masonry unit and the mortar layer. In structural engineering, this bond is not viewed as a simple surface adhesive film; rather, it is a complex, multi-phase composite zone that governs the transfer of tensile and shear stresses across structural joints. Historically, researchers have established that the masonry bond is achieved through two primary concurrent mechanisms: chemical adhesion and mechanical interlocking (Lawrence & Cao, 1987).

Chemical adhesion occurs as the cementitious matrix undergoes hydration, generating crystalline phases that bond with the mineral oxides present on the substrate of the masonry unit. Simultaneously, mechanical interlocking happens when the fluid cement paste penetrates the open capillary pores of the brick surface. As the hydration reactions progress, these interlocking microscopic anchors crystallize within the pores, locking the mortar matrix into the brick surface.

The efficiency of both mechanisms is heavily dictated by the rheological properties of the fresh mortar and the surface texture of the brick. Granular configurations, surface roughness, and pore size distribution determine whether the fresh paste can establish intimate contact with the unit before the onset of initial setting.

The fundamental catalyst governing the transition of fresh mortar into a bound structural system is the moisture transport that occurs immediately upon contact between the two phases. When a wet, plastic mortar is applied to a dry, porous masonry unit, a hydraulic gradient is instantly established. The masonry unit acts as a capillary suction pump, drawing water, dissolved calcium ions, and fine binder particles out of the fresh mortar matrix (Costigan & Pavía, 2013). This phenomenon is physically characterized by the Initial Rate of Absorption (IRA) of the brick.

2.1 Properties of Sourced Commercial Bricks

The mechanical performance and durability of a masonry assembly are heavily influenced by the physical and microstructural characteristics of its masonry units. In contemporary construction, the market has shifted from a reliance on traditional fired clay units to a diverse selection of alternative materials, such as fly ash bricks and Autoclaved Aerated Concrete (AAC) blocks (Venkatarama Reddy & Gupta, 2008).

The primary physical parameter that distinguishes these commercial units is their internal pore architecture, which is categorized into total porosity and pore size distribution. Fired clay bricks possess a complex pore system governed by the mineral composition of the source clay and the peak firing temperatures in local kilns. Generally, higher firing temperatures induce partial vitrification, which reduces total porosity but increases the proportion of large capillary pores (1µm to 10µm), which are highly active in capillary suction (Costigan & Pavía, 2013).

In contrast, non-clay units like fly ash bricks exhibit a denser, more uniform distribution of micro-pores resulting from the compaction and pozzolanic reactions of industrial byproducts.

2.2 Performance of Modern Commercial Cements

The binding phase within masonry mortar is governed by the chemical composition and hydration kinetics of the chosen cement type. In contemporary infrastructure development, the construction sector has increasingly transitioned from traditional Ordinary Portland Cement (OPC) to industrial blended hydraulic cements, specifically Portland Pozzolana Cement (PPC) and Portland Slag Cement (PSC) (Venkatarama Reddy & Gupta, 2008). The fundamental distinction between these modern commercial cements lies in their chemical phase evolution during hydration.

When OPC (typically Grade 53) mixes with water, the primary clinker phases—tricalcium silicate (C_3S) and dicalcium silicate (C_2S)—undergo rapid exothermic hydrolysis. This reaction yields amorphous calcium silicate hydrate (C-S-H) gel, which serves as the primary strength-imparting framework, alongside a substantial byproduct of crystalline calcium hydroxide ($Ca(OH)_2$, or portlandite) and ettringite. The hydration of OPC is characterized by an intensive early heat release and accelerated early strength gain, establishing a rigid crystalline matrix within the initial 3 to 7 days.

2.3 Comparative Macro-Mechanical Performance in Masonry Joints

The micro-level phase modifications induced by these different commercial cements dictate the ultimate macro-mechanical bond capacities of the joint when subjected to external loading regimes. OPC mortars consistently demonstrate rapid early-stage mechanical properties, achieving high compressive and initial bond strengths within the first week of curing. This rapid strength development makes OPC popular for fast-paced construction schedules; however, its tendency to form a brittle, porous ITZ often results in lower long-term flexural tensile and shear bond strengths, with a strong tendency toward sudden adhesive failure along the contact plane (Mojsilović, 2011).

In contrast, masonry joints constructed using PPC and PSC typically display lower initial bond capacities but exhibit substantial strength development over time. By the 28-day milestone, the pozzolanic densification of the ITZ allows blended cement mortars to match or exceed the flexural tensile bond strength (f_{tb}) and the initial shear cohesion (τ_0) of OPC counterparts, provided that proper curing moisture has been maintained (Lumantarna et al., 2014).

2.4 Objectives of the Research Work

In order to address the identified research gaps and systematically evaluate the composite mechanics of the masonry systems, the following core objectives have been established for this thesis:

i. **To characterize the physical and rheological properties of constituent materials:** Quantify the engineering properties of sourced Godavari River sand according to IS 2386, and evaluate the fresh-state consistency and flow values of Ordinary Portland Cement (OPC Grade 53), Portland Pozzolana Cement (PPC), and Portland Slag Cement (PSC) mortar mixes under a standardized water-to-cement ratio of 0.55.

ii. **To evaluate the macro-mechanical performance through a full factorial design:** Construct and structurally test composite masonry assemblages across a 3 x 3 full factorial matrix to determine the ultimate axial compressive strength using three-brick-high stacked prisms (ASTM C1314) and flexural tensile bond strength using five-brick-high bond-wrench assemblies (ASTM C1072).

iii. **To quantify factor significance and material interactions using ANOVA:** Perform a Two-Way Analysis of Variance (ANOVA) on the compiled mechanical test results to statistically isolate the individual contributions and interactive effects of the independent variables (masonry unit types and commercial cement binders) on the global capacity of the masonry joint.

iv. **To analyze the microstructural phase configurations at the interface:** Extract pristine micro-specimens from the failed boundary layers and conduct X-ray Diffraction (XRD) analysis to identify crystalline hydration phases (such as portlandite orientation and ettringite growth) and evaluate the quality of secondary C-S-H gel development within the Interfacial Transition Zone (ITZ).

3. PROCUREMENT AND MATERIAL CHARACTERIZATION

3.1 Selection of Sourced Masonry Units from Amalapuram Region

To ensure this research reflects the actual engineering and construction landscape of the Konaseema district in Andhra Pradesh, all masonry components were procured directly from active commercial supply chains, local kilns, and structural suppliers operating within the Amalapuram region. Sourcing materials from this specific geographic zone is highly significant due to the regional availability of alluvial deltaic soils along the Godavari River basin, which heavily dictates the mineralogical and physical properties of local fired clay products.

3.2 Technical Specifications of Procured Commercial Cements

A. Ordinary Portland Cement (OPC, Grade 53): The procured OPC complies with standard structural specifications for high-strength hydraulic binders. This commercial cement is selected to establish a baseline mortar matrix characterized by rapid hydration kinetics. These binders represent the standard structural products distributed by major national brands (UltraTech Cements) through wholesale building material agencies located within Amalapuram.

B. Portland Pozzolana Cement (PPC, Fly Ash-Based)

The procured PPC is an intimately blended hydraulic cement produced by intergrinding standard Portland clinker with gypsum and a specified percentage of high-quality, reactive pozzolanic materials (pulverized fly ash). PPC is highly popular in coastal and deltaic zones like Amalapuram due to its enhanced resistance to moisture ingress and chemical attack.

C. Portland Slag Cement (PSC)

To evaluate an alternative blended binder system, commercial PSC was procured. This cement is manufactured by intergrinding Portland cement clinker, gypsum, and granulated blast-furnace slag (GGBS), an industrial byproduct of iron manufacturing and this has been purchased from JSW cement company suppliers.

3.3 Physical Dimensions and Geometric Tolerances

A fundamental step in evaluating the structural performance of masonry joints involves quantifying the physical dimensions and geometric consistency of the procured masonry units. Variations in brick dimensions directly influence the uniformity of mortar joint thicknesses, which can alter the distribution of internal stresses when the assembly is loaded.

Table 1: Measured Physical Dimensions and Dimensional Consistency of Sourced Bricks

Brick Variant	Average Length (L, mm)	Average Width (W, mm)	Average Height (H, mm)	Dimensional Consistency
Wire-Cut Clay Bricks	228.4 (±5)	106.2 (±5)	74.5 (±5)	High (Mechanized Extrusion)
Country/Handmade Bricks	221.5 (±3)	102.1 (±3)	68.2 (±3)	Low (Manual Open-Clamp Kiln)
Fly Ash Bricks	229.1 (±5)	109.4 (±3)	75.2 (±3)	Very High (Hydraulic Pressing)

3.4 Compressive Strength of Sourced Masonry Units

The compressive strength of masonry units is a foundational engineering property that dictates the ultimate load-bearing capacity of a composite masonry structure. While the bond strength at the interface governs the resistance to tensile and shear failures, the compressive strength of the individual bricks establishes the upper bound of the masonry assembly's performance under axial compression.

To determine this property, destructive compressive testing was performed on the commercially procured brick variants from the Amalapuram region in strict accordance with standard protocols (ASTM C67/C67M-20; IS 3495-Part 1).

The individual approximate values, computed averages, and typical structural failure modes observed during testing are compiled in Table 2.

Table 2: Compressive Strength Values and Statistical Averages for Sourced Bricks

Brick Variant	Specimen1 (f_b, /mm^2)	Specimen 2 (f_b, /mm^2)	Specimen 3 (f_b, /mm^2)	Specimen 4 (f_b, /mm^2)	Specimen 5 (f_b, /mm^2)	Average Strength ($f_{b,avg}$, N/mm^2)	Primary Structural Failure Mode
Machine-Made Bricks	11.20	9.80	10.50	12.10	11.40	11.00	Clean vertical splitting; minimal crumbling.
Handmade Bricks	3.40	4.80	3.10	4.20	3.50	3.80	Premature shear cracking; high crumbling.
Fly Ash Bricks	8.20	7.60	8.90	7.80	8.50	8.20	Brittle hourglass failure; uniform cracks.

3.5 Initial Rate of Absorption (IRA)

To characterize these absorption properties for the materials sourced from the Amalapuram region, standard laboratory testing was performed on five individual specimens for each of the three active brick categories: handmade clay bricks, machine-made (wire-cut) clay bricks, and fly ash bricks. The testing protocols followed the specifications outlined in ASTM C67/C67M-20 and IS 3495-Part 2.

For the IRA evaluation, dry specimens were partially submerged in a specialized water bed to a depth of precisely 3 mm for exactly 1 minute. The net weight gain (M) due to capillary suction was recorded. The IRA value was determined using the formula:

$$IRA = \frac{M_t}{a\,d}$$

Where,
M_t is the change in specimen mass in g
a is the area of surface of the specimen in mm^2
d is the Density of water in g/mm^3

Table 3: Initial Rate of Absorption (IRA) values of Sourced Bricks

Brick Variant	Specimen 1 IRA (mm)	Specimen 2 IRA (mm)	Specimen 3 IRA (mm)	Specimen 4 IRA (mm)	Specimen 5 IRA (mm)	Average IRA (mm)
Machine-Made Bricks	0.547	0.493	0.573	0.503	0.550	**0.533**
Handmade Bricks	1.403	1.620	1.317	1.540	1.470	**1.470**
Fly Ash Bricks	0.373	0.327	0.413	0.350	0.387	**0.370**

3.6 Water Absorption of Sourced Masonry Units

The total water absorption capacity of a masonry unit serves as a critical indicator of its internal open-pore volume and long-term durability. Unlike the dynamic, early-stage capillary actions measured by the Initial Rate of Absorption (IRA), the 24-hour submersion test quantifies the maximum moisture storage capacity of the mature brick substrate.

$$\text{Water Absorption (\%)} = \left(\frac{W_s - W_d}{W_d}\right) \times 100$$

Where,
W_d dry specimens were weighed,
W_s is the wiped surface-dry

The experimental results, computed averages, and structural behaviors are compiled in Table 4.

Table 4: 24-Hour Gravimetric Water Absorption Values and Averages

Brick Variant	Specimen 1 (%)	Specimen 2 (%)	Specimen 3 (%)	Specimen 4 (%)	Specimen 5 (%)	Average Absorption (%)
Machine-Made Bricks	12.10	11.50	13.00	11.80	12.60	12.20%
Handmade Bricks	18.50	21.40	17.90	20.20	19.50	19.50%
Fly Ash Bricks	9.20	8.60	9.90	8.90	9.40	9.20%

The experimental results demonstrate distinct variations in moisture capacity that directly reflect the manufacturing methods used by local suppliers. The traditional country/handmade clay bricks exhibited the highest average water absorption capacity (19.50%). This highly porous behavior is justified by the manual molding process and the lower, non-uniform temperatures characteristic of local open-clamp kilns.

3.7 Fresh Mortar Properties: Consistency, and Flow Value

Three key fresh properties were evaluated across the three distinct cement options (OPC Grade 53, PPC, and PSC) combined with Godavari River sand: consistency and flow value.

i. **Consistency:** Measured via the standard plunger penetration apparatus conforming to **IS 2250-1981**, consistency quantifies the relative fluidity and initial stiffness of the mix.

ii. **Flow Value:** Determined using a standard flow table assembly (**IS 5512-1983**; **ASTM C1437-20**), this metric assesses the workability and spreadability of the mortar when subjected to a controlled dropping impact.

Table 5: Fresh-State Rheological Profiles of Different Commercial Cement Mixes

Cement Mix Type (1:3 Ratio with River Sand)	Rheological Property Evaluated	Trial 1	Trial 2	Trial 3	Average Value	Target Engineering Standards / Specifications
OPC Grade 53 Mix	Consistency / Penetration (mm)	32.50	30.00	31.10	31.20 mm	IS 2250-1981 / ASTM C270:
	Flow Value (%)	112.0	109.0	110.0	110.3%	Flow target: 110% ± 5%.
PPC (Fly Ash-Based) Mix	Consistency / Penetration (mm)	34.20	32.80	33.50	33.50 mm	IS 2250-1981 / ASTM C270:
	Flow Value (%)	114.0	109.0	112.0	111.7%	Flow target: 110% ± 5%.
PSC (Slag-Based) Mix	Consistency / Penetration (mm)	31.80	29.50	31.10	30.80 mm	IS 2250-1981 / ASTM C270:
	Flow Value (%)	111.0	106.0	108.0	108.3%	Flow target: 110% ± 5%.

4. EXPERIMENTAL RESULTS FOR MECHANICAL PROPERTIES

4.1.1 Full Factorial Experimental Design Matrix

The testing matrix evaluates three distinct brick variants sourced from the Amalapuram region: country/handmade clay bricks, machine-made (wire-cut) clay bricks, and pressed fly ash bricks. These units are paired across all combinations with three commercial cement types: Ordinary Portland Cement (OPC Grade 53), Portland Pozzolana Cement (PPC), and Portland Slag Cement (PSC).

To isolate the material compatibility factors, control parameters were standardized across all fabricated assemblages. A consistent water-to-cement (w/c) ratio of 0.55 was maintained for all mortar mixes, utilizing a 1:3 dry volumetric binder-to-river sand ratio. All specimens were constructed with a uniform mortar joint thickness of 10 mm ± 1 mm and subjected to a standardized wet-curing regime for a curing age of precisely 28 days before destructive mechanical testing (IS 2250-1981). The resulting 3 x 3 full factorial design yields 9 unique material combinations, with 3 replicates prepared per cell to ensure statistical validity, as detailed in Table 6.

4.1.2Testing of Compressive Strength Prisms

For the compressive testing series, standard three-brick-high stacked prisms were constructed to assess axial capacity (ASTM C1314-21). A level steel platform served as the baseline jig. The first brick was aligned horizontally, and a uniform layer of fresh mortar was spread over its bedding face. Non-deformable gauge spacers were placed at the corners to guarantee a precise mortar joint thickness of 10 mm. The second brick was positioned directly above the first, and a downward vertical pressure was applied until the mortar compressed exactly to the 10 mm spacer boundary. Excess mortar squeezing out of the joint was struck off flush with a trowel.

This process was repeated for the third course. A vertical spirit level confirmed perpendicular alignment across all 3 replicates per mix to eliminate eccentric loading risks.

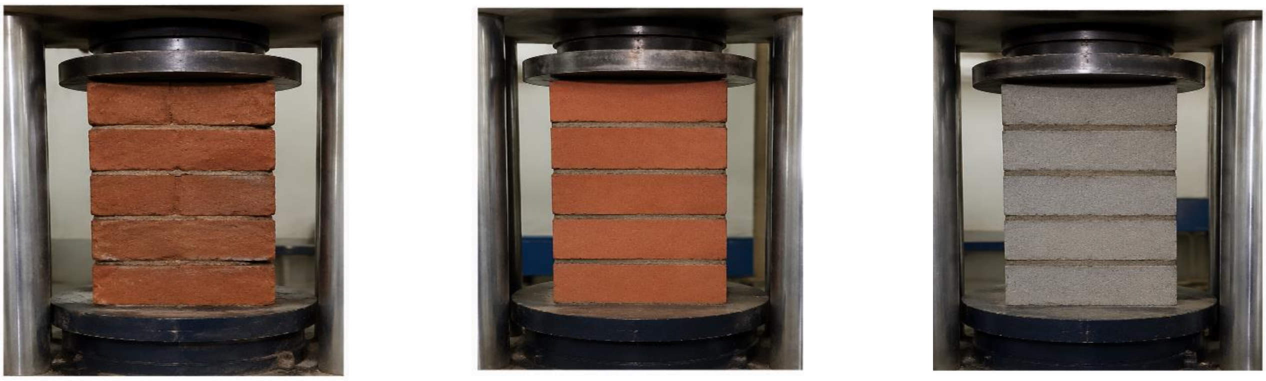

Fig. 1 a) Handmade red cly brick masonry (5 layers)

Fig. 1 b) Machine-made red cly brick masonry (5 layers)

Fig. 1 c) Fly ash brick masonry (5 layers)

The individual compressive values (f'_m) obtained from three distinct replicates for each full factorial cell are detailed in Table 6.

Table 6: 28-Day Compressive Strength Test Results for Masonry Prisms (f'_m, N/mm^2)

Mix Design ID	Masonry Unit Type	Cement Binder Variant	Replicate 1	Replicate 2	Replicate 3	Average f'_m
HM-OPC	Country/Handmade Brick	OPC Grade 53	2.45	2.10	2.35	2.30
HM-PPC	Country/Handmade Brick	Portland Pozzolana	2.85	2.60	2.95	2.80
HM-PSC	Country/Handmade Brick	Portland Slag Cement	2.65	2.40	2.45	2.50
MM-OPC	Machine-Made Brick	OPC Grade 53	6.20	5.80	6.00	6.00
MM-PPC	Machine-Made Brick	Portland Pozzolana	6.80	6.45	6.55	6.60
MM-PSC	Machine-Made Brick	Portland Slag Cement	6.40	6.10	6.40	6.30
FA-OPC	Pressed Fly Ash Brick	OPC Grade 53	4.40	4.15	4.35	4.30
FA-PPC	Pressed Fly Ash Brick	Portland Pozzolana	4.95	4.65	4.80	4.80
FA-PSC	Pressed Fly Ash Brick	Portland Slag Cement	4.60	4.45	4.45	4.50

To confirm the statistical validity of these values, a Two-Way ANOVA with replication was conducted at a 95% confidence interval (α= 0.05). The resulting variance data is compiled in Table 7.

Table 7: Two-Way ANOVA Table for Masonry Compressive Strength

Source of Variation	Sum of Squares (SS)	Degrees of Freedom (df)	Mean Square (MS)	Computed F-Value	p-value	F_{crit} Significance
Masonry Units (A)	64.980	2	32.490	1265.87	< .00001	3.55 (Significant)
Cement Binders (B)	1.820	2	0.910	35.46	< .00001	3.55 (Significant)

Interaction (A X B)	0.260	4	0.065	2.53	0.07730	2.93 (Not Signif.)
Error (Internal)	0.462	18	0.026	-	-	-
Total Variation	67.522	26	-	-	-	-

The statistical breakdown confirms that Masonry Unit Type exerts the dominant control over compressive strength, yielding an exceptionally high F-value (1265.87). This behavior is justified because the ultimate load capacity of a prism depends heavily on the lateral confinement mechanics between the mortar and the unit. The higher tensile strength and structural density of machine-made bricks (11.00 N/mm^2 unit strength) resist lateral tension far better than traditional handmade units (3.80 N/mm^2 unit strength), preventing early vertical splitting (Costigan & Pavía, 2013).

4.1.3 Flexural Tensile Bond Strength of Masonry

Interfacial tensile bond strength was quantified using standard five-brick-high bond-wrench assemblies tested at a 28-day curing age (ASTM C1072-19). This test evaluates the adhesive capacity of the joint plane. The individual failure values (f_{bt}) recorded across three replicates are structured in Table 8.

Table 8: 28-Day Flexural Tensile Bond Strength Test Results (f_{bt}, N/mm^2)

Mix Design ID	Masonry Unit Type	Cement Binder Variant	Replicate 1	Replicate 2	Replicate 3	Average f_{bt}, N/mm^2
HM-OPC	Country/Handmade Brick	OPC Grade 53	0.14	0.11	0.11	0.12
HM-PPC	Country/Handmade Brick	Portland Pozzolana	0.25	0.21	0.23	0.23
HM-PSC	Country/Handmade Brick	Portland Slag Cement	0.19	0.16	0.16	0.17
MM-OPC	Machine-Made Brick	OPC Grade 53	0.38	0.34	0.36	0.36
MM-PPC	Machine-Made Brick	Portland Pozzolana	0.54	0.49	0.53	0.52
MM-PSC	Machine-Made Brick	Portland Slag Cement	0.46	0.41	0.42	0.43
FA-OPC	Pressed Fly Ash Brick	OPC Grade 53	0.22	0.18	0.20	0.20
FA-PPC	Pressed Fly Ash Brick	Portland Pozzolana	0.34	0.30	0.32	0.32
FA-PSC	Pressed Fly Ash Brick	Portland Slag Cement	0.28	0.24	0.26	0.26

The corresponding Two-Way ANOVA evaluations for the flexural tensile data are detailed in Table 9.

Table 9: Two-Way ANOVA Table for Masonry Flexural Tensile Bond Strength

Source of Variation	Sum of Squares (SS)	Degrees of Freedom (df)	Mean Square (MS)	Computed F-Value	p-value	Fcrit Significance
Masonry Units (A)	0.3456	2	0.1728	493.71	< .00001	3.55 (Significant)
Cement Binders (B)	0.0936	2	0.0468	133.71	< .00001	3.55 (Significant)
Interaction (A x B)	0.0096	4	0.0024	6.86	0.00154	2.93 (Significant)
Error (Internal)	0.0063	18	0.00035	-	-	-
Total Variation	0.4551	26	-	-	-	-

The tensile analysis reveals significant interaction kinetics ($F = 6.86 > F_{crit}$). While the brick variant continues to govern the primary variance due to surface profile and texture variations (Oliveira et al., 2012), the chemical and physical characteristics of the cement play a critical role.

The machine-made wire-cut brick paired with PPC achieved the highest bond performance (0.52 N/mm^2). This outcome is justified by the balanced initial capillary suction of the extruded clay surface drawing in the highly refined, pozzolanic micro-particles. This process enhances structural mechanical interlocking within the Interfacial Transition Zone (ITZ) (Lawrence & Cao, 1987).

5. SAMPLING AND PREPARATION OF INTERFACIAL MICRO-SPECIMENS FOR X-ray DIFFRACTION ANALYSIS

The sampling program focused on two high-contrast boundary profiles prepared with Ordinary Portland Cement (OPC Grade 53) mortar at a water-to-cement (w/c) ratio of 0.55:

- **Profile 1:** Machine-Made Clay Brick coupled with OPC-53 mortar (MM-OPC)
- **Profile 2:** Fly Ash Brick coupled with OPC-53 mortar (FA-OPC)

5.1 Precision Diamond Sectioning and Stabilization Mechanics

The step-by-step extraction protocol was executed under strict laboratory configurations to maintain the pristine state of the fractured contact planes. Immediately following destructive bond-wrench testing, specimen blocks containing intact remnants of the joint interface were transferred to a precision specimen preparation laboratory. The extraction workflow proceeded through four distinct phases:

Phase 1: Low-Speed Diamond Saw Slicing

To minimize structural disruption to the delicate contact zone, the bulk masonry fragments were mounted in the clamping vice of a low-speed precision diamond sectioning saw. Slicing was executed using a high-concentration diamond wafering blade rotating at a controlled velocity of 150 rpm.

To completely avoid structural alterations of heat-sensitive hydration phases such as gypsum reformation from ettringite or portlandite carbonation traditional water-based coolants were replaced with a non-aqueous, mineral-oil-based lubricating fluid. Cubical micro-specimens measuring approximately 10 mm x 10 mm x 5 mm were carefully extracted, ensuring the original failure plane occupied the geometric center of the cube.

Phase 2: Epoxy Vacuum Impregnation

For samples intended for intact cross-sectional analysis, the fragile extracted cubes were immediately placed into silicone molds and subjected to vacuum impregnation using an ultra-low-viscosity, clear epoxy resin. The specimens were held under a vacuum of 0.1 MPa for 30 minutes, forcing the liquid polymer deep into the open capillary voids and micro-cracks of the ITZ. This epoxy support framework mechanically locked the hydration products and the brick matrix together, ensuring that subsequent polishing steps would not pluck out brittle crystals like ettringite or portlandite (Oliveira et al., 2012).

Phase 3: Solvent-Based Dehydration

To arrest ongoing cement hydration without collapsing the delicate calcium silicate hydrate (C-S-H) gel structures, the extracted fragments were subjected to solvent exchange. The specimens were submerged in high-purity isopropanol (>99.9% concentration) for a continuous period of 7 days. The alcohol molecules progressively replaced the free pore water within the matrix without stripping the chemically bound water from the crystalline hydrates, stabilizing the phase composition for high-vacuum analytical environments.

Phase 4: Low-Energy Mechanical Pulverization

For X-ray Diffraction (XRD) phase identification, the intact interface boundary layer (extending roughly 1 mm from the true fracture line) was carefully isolated using a micro-chisel under an optical stereomicroscope. These localized scrapings were then pulverized using a low-energy agate mortar and pestle. Grinding was strictly limited to short, intermittent bursts to prevent mechanical amorphization of the crystalline components. The resulting analytical powders were passed completely through a 45μm (No. 325) standard sieve, satisfying the grain-size criteria required to eliminate preferred orientation errors during X-ray diffraction tracking.

5.2 X-ray Diffraction (XRD) Analysis of the Contact Layer

5.2.1 Instrumentation Parameters and Mineralogical Tracking

The quantitative mineralogical composition at the isolated interface contact layer was mapped using an advanced, high-resolution X-ray Diffractometer. The instrument was configured with a copper target source generating Cu-Kα ($\lambda = 1.5418$), operated at an accelerating potential of 40 kV and a tube current of 40 mA.

To capture both highly crystalline tracking planes and diffuse, semi-amorphous mineral fields, scanning was executed continuously across a wide angular range from $2\Theta = 5°$ to $2\Theta = 70°$. A fine step size of 0.02° (2Θ) combined with an exposure time of 2.0 seconds per step was selected to ensure high signal-to-noise ratios.

Phase identification and peak indexing were performed using specialized powder diffraction software paired with the International Centre for Diffraction Data (ICDD) database. The primary mineralogical target phases tracked at the interface included:

- **Portlandite ($Ca(OH)_2$):** Tracked via its principal diagnostic reflections at 2Θ = 18.1° (001 plane) and 2Θ = 34.1° (101 plane).
- **Ettringite ($C_{a6}Al_2SO_4)_3$ $(OH)_{12}$ .26 (H_2O):** Identified via its signature low-angle peaks at 2Θ= 9.1° (100) and 2Θ= 15.8° (110).
- **Quartz (SiO_2):** Originating from the river sand and clay brick bodies, displaying intense reflections at 2Θ = 20.8° and 2Θ = 26.6°.
- **Calcium Silicate Hydrate (C-S-H) Gel Quality:** Evaluated by observing the broad, diffuse amorphous humps distributed between 2Θ = 28° and 2Θ = 35°.

The structural and mineralogical variations revealed by XRD analysis provide a clear explanation for the macro-mechanical behaviors observed in Chapter 4.

In the MM-OPC assemblage, the machine-made clay brick presents a chemically inert, vitreous surface with a balanced initial rate of absorption (IRA = 0.533 mm). When the fresh OPC-53 paste meets this boundary, a localized film of water forms against the impervious clay surface, a phenomenon known as the "wall effect" (Costigan & Pavía, 2013).

Because OPC-53 hydrates rapidly without any pozzolanic additions, calcium ions quickly saturate this interfacial water film. This allows large, weak crystals of portlandite to nucleate and grow with their cleavage planes oriented parallel to the brick surface. This accumulation of oriented portlandite, combined with standard ettringite growth, creates a distinct structural zone that is more prone to cleavage failure under flexural tensile loads.

In the FA-OPC assemblage, the pressed fly ash brick does not behave as a chemically inert substrate. Although the binder utilized is pure OPC-53, the brick surface itself contains a high volume of reactive, amorphous pozzolanic silica (SiO_2) and alumina (Al_2O_3).

6. Conclusions

A 3 × 3 full factorial experimental design was used to study the effects of different types of bricks and commercial cement binders on the strength of masonry. This design helped in identifying both the individual effects of each factor and their combined influence on masonry performance.

To ensure a fair comparison, all masonry specimens were prepared under the same conditions. A water–cement ratio of 0.55, a 1:3 cement–sand mortar mix, a 10 mm mortar joint thickness, and 28 days of curing were maintained throughout the study. Therefore, any differences in strength were mainly due to the type of brick and cement used.

❖ **Conclusions from ANOVA Results**

✓ **Effect of Brick Type on Compressive Strength**
The ANOVA results showed that the type of brick had the greatest influence on the compressive strength of masonry (F = 1265.87). Machine-made wire-cut bricks produced much stronger masonry than handmade clay bricks because of their higher strength, better dimensional accuracy, and ability to resist cracking under load.

✓ **Effect of Cement Type**
The type of cement also had a significant effect on compressive strength (F = 35.46). Masonry constructed with Portland Pozzolana Cement (PPC) mortar showed the highest compressive strength. This improvement is mainly due to the pozzolanic reaction, which produces additional calcium silicate hydrate (C–S–H) gel and makes the mortar denser and stronger.

✓ **Combined Effect of Brick and Cement**
The ANOVA results for flexural bond strength showed a significant interaction between brick type and cement type (F = 6.86). This indicates that bond strength depends not only on the properties of the brick or mortar individually but also on how well they work together at the brick–mortar interface. Good compatibility between the two materials results in stronger bonding.

❖ **Conclusions from X-Ray Diffraction (XRD) Analysis**

✓ **Portlandite Formation at the Clay Brick Interface (MM–OPC)**
The XRD analysis of machine-made clay brick masonry prepared with OPC mortar showed strong portlandite ($Ca(OH)_2$) peaks at 18.15° and 34.11° (2θ). The sharp peaks indicate the formation of large and well-developed calcium hydroxide crystals along the brick–mortar interface. These crystals create a weak layer that can reduce the bond strength.

✓ **Pozzolanic Reaction at the Fly Ash Brick Interface (FA–OPC)**
For fly ash brick masonry, the XRD results showed much smaller portlandite peaks. This indicates that the silica and alumina present in the fly ash brick reacted with calcium hydroxide through the pozzolanic reaction, reducing the amount of weak portlandite at the interface.

✓ **Formation of a Denser Bonding Layer**

The reduction in portlandite was accompanied by the formation of additional calcium silicate hydrate (C–S–H) gel, as indicated by the broad XRD hump between 28° and 35° (2θ). This newly formed C–S–H filled pores and improved the density of the brick–mortar interface, resulting in stronger chemical bonding and better overall masonry performance.

ACKNOWLEDGMENT

The authors express their sincere gratitude to Bonam Venkata Chalamayya Engineering College for providing the laboratory facilities, infrastructure, technical support, and academic environment necessary for carrying out this research work.

REFERENCES

1. ASTM International. (2019). Standard specification for mortar for unit masonry (ASTM C270-19ae1). West Conshohocken, PA: ASTM International.
2. ASTM International. (2019). Standard test methods for measurement of masonry flexural bond strength (ASTM C1072-19). West Conshohocken, PA: ASTM International.
3. ASTM International. (2020). Standard test methods for sampling and testing brick and structural clay tile (ASTM C67/C67M-20). West Conshohocken, PA: ASTM International.
4. ASTM International. (2020). Standard test method for flow of hydraulic cement mortar (ASTM C1437-20). West Conshohocken, PA: ASTM International.
5. ASTM International. (2021). Standard test method for compressive strength of masonry prisms (ASTM C1314-21). West Conshohocken, PA: ASTM International.
6. Bureau of Indian Standards. (1963). Methods of test for aggregates for concrete: Part 1—Particle size and shape (IS 2386-Part 1). New Delhi, India: BIS.
7. Bureau of Indian Standards. (1963). Methods of test for aggregates for concrete: Part 3—Specific gravity, density, voids, absorption (IS 2386-Part 3). New Delhi, India: BIS.
8. Bureau of Indian Standards. (1965). Specification for sand for masonry mortars (IS 2116). New Delhi, India: BIS.
9. Bureau of Indian Standards. (1981). Code of practice for preparation and use of masonry mortars (IS 2250-1981). New Delhi, India: BIS.
10. Bureau of Indian Standards. (1983). Specification for flow table for use in tests of hydraulic cements and pozzolanic materials (IS 5512-1983). New Delhi, India: BIS.
11. Bureau of Indian Standards. (1987). Code of practice for structural use of unreinforced masonry (IS 1905-1987). New Delhi, India: BIS.
12. Bureau of Indian Standards. (2016). Coarse and fine aggregates for concrete—Specification (IS 383). New Delhi, India: BIS.
13. Bureau of Indian Standards. (2019). Methods of tests of burnt clay building bricks (IS 3495 Parts 1–4). New Delhi, India: BIS.
14. Bureau of Indian Standards. (2019). Methods of tests of burnt clay building bricks—Part 1: Determination of compressive strength (IS 3495-Part 1). New Delhi, India: BIS.
15. Costigan, A., & Pavía, S. (2013). Investigation of the intrinsic characteristics of bricks and mortars or how they affect the bond strength of masonry. Journal of Materials in Civil Engineering, 25(11), 1649–1656.
16. European Committee for Standardization. (2002). Methods of test for masonry—Part 3: Determination of initial shear strength (EN 1052-3:2002). Brussels, Belgium: CEN.
17. Grandet, J., & Ollivier, J. P. (1980). Orientation des cristaux d'hydroxyde de calcium au contact des granulats dans les mortiers. Cement and Concrete Research, 10(6), 759–767.
18. Lawrence, S. J., & Cao, H. T. (1987). An experimental study of the interface between brick and mortar. Proceedings of the 8th International Brick/Block Masonry Conference, 348–353.
19. Lumantarna, R., Biggs, D. T., & Ingham, J. M. (2014). Compressive, tensile, and shear bond strength of unreinforced masonry sampled from New Zealand buildings. Journal of Materials in Civil Engineering, 26(4), 631–640.
20. Mojsilović, N. (2011). Tensile bond strength of masonry: An experimental study. Materials and Structures, 44(4), 833–843.
21. Oliveira, D. V., Silva, R. A., Garbin, E., & Lourenço, P. B. (2012). Fracture behavior of bond between brick and mortar. Construction and Building Materials, 35, 784–791.
22. Sarangapani, G., Venkatarama Reddy, B. V., & Jagadish, K. S. (2005). Brick-mortar bond and masonry compressive strength. Journal of Materials in Civil Engineering, 17(2), 229–237.